Biochimica et Biophysica Acta 1840 (2014) 262–270

Contents lists available at ScienceDirect

Biochimica et Biophysica Acta

journal homepage: www.elsevier.com/locate/bbagen

PDT-induced epigenetic changes in the mouse cerebral cortex: A protein microarray study

S.V. Demyanenko [a], A.B. Uzdensky [a,*], S.A. Sharifulina [a], T.O. Lapteva [b], L.P. Polyakova [c]

[a] Southern Federal University, Rostov-on-Don 344090, Russia
[b] Regional Consulting and Diagnostic Center, Rostov-on-Don 344010, Russia
[c] Rostov State Medical University, Rostov-on-Don 344022, Russia

ARTICLE INFO

Article history:
Received 26 May 2013
Received in revised form 2 August 2013
Accepted 11 September 2013
Available online 17 September 2013

Keywords:
ALA-PDT
Brain cortex
Proteomic
Epigenetic
Antibody microarray

ABSTRACT

Background: Photodynamic therapy (PDT) is used for cancer treatment including brain tumors. But the role of epigenetic processes in photodynamic injury of normal brain tissue is unknown.
Methods: 5-Aminolevulinic acid (ALA), a precursor of protoporphyrin IX (PpIX), was used to photosensitize mouse cerebral cortex. PpIX accumulation in cortical tissue was measured spectrofluorometrically. Hematoxylin/eosin, gallocyanin–chromalum and immunohistochemical staining were used to study morphological changes in PDT-treated cerebral cortex. Proteomic antibody microarrays were used to evaluate expression of 112 proteins involved in epigenetic regulation.
Results: ALA administration induced 2.5-fold increase in the PpIX accumulation in the mouse brain cortex compared to untreated mice. Histological study demonstrated PDT-induced injury of some neurons and cortical vessels. ALA-PDT induced dimethylation of histone H3, upregulation of histone deacetylases HDAC-1 and HDAC-11, and DNA methylation-dependent protein Kaiso that suppressed transcriptional activity. Upregulation of HDAC-1 and H3K9me2 was confirmed immunohistochemically. Down-regulation of transcription factor FOXC2, PABP, and hBrm/hsnf2a negatively regulated transcription. Overexpression of phosphorylated histone H2AX indicated activation of DNA repair, but down-regulation of MTA1/MTA1L1 and PML — impairment of DNA repair. Overexpression of arginine methyltransferase PRMT5 correlated with up-regulation of transcription factor E2F4 and importin α5/7.
Conclusion: ALA-PDT injures and kills some but not all neurons and caused limited microvascular alterations in the mouse cerebral cortex. It alters expression of some proteins involved in epigenetic regulation of transcription, histone modification, DNA repair, nuclear protein import, and proliferation.
General significance: These data indicate epigenetic markers of photo-oxidative injury of normal brain tissue.

1. Introduction

Photodynamic therapy (PDT) based on photogeneration of highly cytotoxic singlet oxygen and following development of oxidative stress that leads to death of stained cells is currently used in oncology [1]. Protoporphyrin IX (PpIX) is a very efficient endogenous photosensitizer. After administration of 5-aminolevulinic acid (ALA), its natural precursor, cells produce PpIX through the heme biosynthetic pathway [2]. ALA-based PDT is currently used for photodynamic diagnosis and therapy of brain tumors [3–6]. However, PDT use for treatment of brain tumors is limited by injury of normal neuronal and glial cells around a tumor that can induce unacceptable neurological disorders and side effects. Therefore, PDT effects on normal nervous tissue should be carefully investigated.

Cell reactions to various impacts including PDT and their death are controlled by the complex signaling system consisting of thousands signaling proteins organized in tens of signaling pathways [7–9]. The first level of intracellular regulation is provided by proteins present in a cell. If their ability is insufficient, additional gene expression and protein synthesis are stimulated. Gene expression is controlled by transcription

Abbreviations: ALA, aminolevulinic acid; AP-1/c-Jun, activation protein transcription factor 1; BACH1, breast cancer type1 protein; CENP-E, centromere protein E; hBrm/hsnf2a, chromatin remodeling factor; E2F4, E2F transcription factor 4; FOXC2, forkhead box C2; G9a, histone methyltransferase G9a; hABH1, human AlkB homolog 1; γH2AX, histone H2AX phosphorylated at serine 139; H3K9me2, histone H3 dimethylated at lysine 9; HDAC-1, HDAC-10 and HDAC-11, histone deacetylases; HDRP, HDAC related protein; MTA1/MTA1L1, metastasis-associated protein 1/metastasis tumor associated 1-like 1; N-CoR, co-repressor complex; PABP, poly(A)-binding protein; PDT, photodynamic therapy; PML, promyelocytic leukemia; PRMT5, protein arginine methyltransferase 5; PpIX, protoporphyrin IX; SIR 2, silent information regulator; SUV39H1, suppressor of variegation 3-9 homolog 1; TXNIP, thioredoxin-interacting protein

* Corresponding author at: Department of Biophysics and Biocybernetics, Southern Federal University, Institute of Neurocybernetics, 194/1 Stachky Ave., NII NK, Rostov-on-Don 344090, Russia. Tel./fax: +7 8632 433577.
E-mail addresses: demyanenkosvetlana@gmail.com (S.V. Demyanenko), auzd@yandex.ru (A.B. Uzdensky), aulova_sveta@mail.ru (S.A. Sharifulina), Lto-96@yandex.ru (T.O. Lapteva), Lpolyakova2013@yandex.ru (L.P. Polyakova).

0304-4165/$ – see front matter © 2013 Elsevier B.V. All rights reserved.
http://dx.doi.org/10.1016/j.bbagen.2013.09.014

factors and epigenetic regulators. Main epigenetic processes include DNA methylation/demethylation, and covalent histone modifications: methylation/demethylation, acetylation/deacetylation, and phosphorylation/dephosphorylation, which regulate access of transcription factors and RNA polymerase II to gene promoters. Aberrant DNA methylation and histone modifications are involved in diverse neuronal functions and neurological disorders such as synaptic plasticity and memory formation [10], Alzheimer, Parkinson, and Huntington diseases [11,12], schizophrenia [13], epilepsy [14] and stroke [14]. However, the role of epigenetic processes in the reactions of the nervous tissue to photodynamic treatment remains unknown.

In the present work we studied ALA-mediated PpIX accumulation in the mouse cerebral cortex tissue, ALA-PDT-induced morphological alterations, and changes in the expression of 112 proteins involved in epigenetic regulation.

2. Materials and methods

2.1. Chemicals

The Panorama Ab Microarray Gene Regulation Kits (GRAA2), CelLytic™ NuCLEAR™ Extraction Kit (NXTRACT), Bradford reagent, anti-HDAC-1 (H3284, Sigma-Aldrich), anti-H3K9me2 (D5567, Sigma-Aldrich), protoporphyrin IX, and 5-aminolevulinic acid hydrochloride were obtained from Sigma-Aldrich Rus (Moscow, Russia). Cy3™ or Cy5™ monofunctional reactive dyes were supplied by GE Healthcare (UK). The test-system REVEAL Polyvalent HRP-DAB Detection System (SPD-060) was supplied by Spring Bioscience (USA).

2.2. Experimental animals

Outbred male mice CD-I (20–25 g) were obtained from the Laboratory of animal breeding at the Institute of Bioorganic Chemistry RAS (Moscow, Russia). The animal holding room was maintained at a constant temperature and humidity, 12-hour light/dark schedule, and an air exchange rate of 18 changes per hour. Animal care protocol corresponded to the institutional guidelines. For the surgical procedures, the mice were anesthetized with intraperitoneally injected (i.p.) sodium thiopental (40 mg/kg). After the experiment, all animals were euthanized with sodium thiopental (120 mg/kg, i.p.). All experimental procedures were conducted in accordance with the European Union guidelines for the use of experimental animals.

2.3. Protoporphyrin IX assay

Experimental mice were i.p. injected with 0.30 ml ALA dissolved in PBS at a dose of 100 mg/kg like that was used for PpIX measurements in glioma-bearing mice [15]. At 4 h after ALA administration, mice were injected with heparin (0.15 ml, 1000 UI) to prevent blood coagulation, perfused with 200 ml of sterile saline, and sacrificed. According to [16,17], the 2 mm thick cerebral cortex slices were homogenized on ice in ethyl acetate:acetic acid mixture (4:1) using consecutively the Potter homogenizer and the ultrasound homogenizer Sonics Vibracell (Sonics and Materials Inc., Newtown, USA). The homogenates were then centrifuged 30 min at 3000 *g*. The supernatants were treated with the equal volume of 5% HCl and centrifuged 2 min at 1400 *g*. The HCl extraction was repeated until no detectable fluorescence remained in the organic layer. PpIX fluorescence spectra were measured at 604 nm (the excitation wavelength 406 nm) using the Hitachi F-4010 spectrofluorometer (Hitachi, Japan). 1 nmol/ml PpIX solution was used as a reference standard.

2.4. Histological study

Animals were sacrificed at 1 or 4 h after ALA-PDT, and their brains were extracted and fixed by 10% buffered formalin (pH 7.2). Paraffin-embedded tissue samples were cross-sectioned by 6–8 μm slices, and mounted on standard microscopic slides. Deparaffinization was accomplished by consecutive immersions in xylene (twice, 3 min each); 100% ethanol (twice, 3 min each); 95% ethanol (twice, 3 min each); and distilled water (3 min). The sections were stained with hematoxylin and eosin. The sections were dehydrated by ethanol (50%, 70%, 80%, 95% × 2, 100% × 2), cleared by xylene (3–4 times), mounted in Canada balsam and examined under the microscope Nikon Eclipse FN1 (Japan). Normal and pathological neurons were counted in the PDT-treated sensomotory mouse cerebral cortex stained with hematoxylin/eosin. All observed neurons were divided into three categories: (1) normal, (2) intermediately damaged (hypochromic or hyperchromic), and (3) pyknotic. Their numbers were counted using an ocular grid (magnification × 400) in six randomized fields in each slide. The average number of neurons per a visual field in PDT-treated mice (1 or 4 h after the treatment, n = 5 in each group) was compared to that in the control group using the Student's *t*-test. Gallocyanin–chromalum staining of deparaffinated slices [18] was used for estimation of the level of nucleic acids in the brain cortex samples.

2.5. Immunohistochemical staining

Mice were perfused transcardially with 4% paraformaldehyde in 0.1 M PBS (pH 7.4) at 1 h after ALA-PDT. The 7 × 7 × 2 mm^3 pieces of the irradiated brain sensomotory cortex were incubated 12 h in this fixative solution and embedded into paraffin. Unmasking of deparaffinated slices was performed in Tween 20-containing Tris-EDTA Buffer (10 mM Tris, 1 mM EDTA, 0.05% Tween 20, pH9.0) in the pressure chamber Pascal (Dako, USA). Slides were triple washed in Tris-buffered saline, pH 7.4 (TBS). The test-system REVEAL Polyvalent HRP-DAB Detection System (SPD-060, Spring Bioscience, USA) was used according to producer recommendations. After washing, slides were incubated 10 min with 200 μl of the Hydrogen Peroxide Block (0.3% H_2O_2, <0.1% sodium azide) at room temperature; washed twice by TBS; incubated 10 min with 200 μl of Protein Block (PBS, pH 7.6, with 0.5% BSA, 0.5% casein, <0.1% sodium azide), and washed twice by TBS. After that, 200 μl solutions of anti-HDAC-1 (H3284, Sigma-Aldrich; 1:700) or anti-H3K9me2 (D5567, Sigma-Aldrich; 1:1500) in PBS were applied for 1 h at 37 °C. After triple washing in TBS, 200 μl of the Complement (Rabbit anti-mouse secondary antibody) was applied for 10 min. After following washing in TBS, the HRP Conjugate (goat anti-rabbit secondary antibody conjugated to horseradish peroxidase) was applied for 15 min. After 4-fold washing in TBS, the mixture of 4 μl of DAB Chromogen (3,3′ Diaminobenzidine chromogen) and 200 μl of DAB Substrate (Substrate buffer, pH 7.5 with hydrogen peroxide) was applied for 3 min. Then the slides were washed 4 times in TBS and stained with Mayer's hematoxylin. Images were photographed on the microscope Nikon Eclipse FN1 (Japan), objective 40×. All analyses were carried out in comparable areas under the same optical and light conditions. The software ImageJ (NIH, USA) was used for image analysis. The RGB splitting revealed the most contrast immune-positive structures in the blue channel. Binary images in this channel showed only the immunopositive structures. The immunoreactivity index was determined like in [19] as:

$$K_i = \sum \text{immunopositive pixels} / \sum \text{total number of pixels} \times 100\%.$$

K_i was determined in 12 sections in each of 3 experimental and 3 control mice. Any significant difference between non-irradiated and animals that were irradiated without ALA administration was not observed (not shown).

2.6. PDT protocol

Four hours after ALA administration (100 mg/kg, i.p), the animals were anesthetized and fixed in the stereotactic frame. After pericranium

removal, the brain was irradiated 20 min by He–Ne laser (633 nm, 15 mW/cm^2; the total PDT dose = 18 J/cm^2) through the cranial bone as in [5,20]. After 1 or 4 h, the mice were perfused with saline, and sacrificed. The 7 × 7 × 2 mm^3 brain cortex slices were quickly weighted, frozen in the liquid nitrogen, and then stored in a freezer at −85 °C.

2.7. Proteomic study

The frozen tissue samples of cerebral cortex were primarily ground in cooled mortars. Then the tissues were homogenized 1 min (20 × 3-second intervals interrupted by 10-second silence intervals) on ice by the ultrasound homogenizer Sonics Vibracell (Sonics and Materials Inc., Newtown, USA) in the Buffer A consisting of the Extraction/Labeling Buffer, a component of GRAA2, supplied with protease and phosphatase inhibitor cocktails and nuclease benzonase. Then the samples were centrifuged 20 min at 10000 rpm in the cooled centrifuge Eppendorf 5417 C/R (Hamburg, Germany). The supernatant that contained mainly cytoplasmic proteins was stored on ice. The precipitate containing cell nuclei was resuspended and incubated 30 min at a room temperature with the Extraction Buffer, NXTRACT component. The lysate containing nuclear proteins was centrifuged 10 min at 14200 rpm. The obtained supernatant was mixed with the equal volume of the cytoplasmic fraction. The experimental (cerebral cortex tissues obtained at 1 or 4 h after ALA-PDT) and control samples were diluted to 1 mg/ml protein content. Experimental and control samples were then incubated 30 min with Cy3 or Cy5 (1 mg/ml), respectively, at a room temperature in the dark. The unbound dye was removed by centrifugation (4000 rpm; 4 min) of the SigmaSpin Columns (GRAA2 components) filled with 200 μl of the labeled protein samples. The eluates were collected, and protein concentration was assayed using Bradford reagent. The samples with the dye-to-protein ratio > 2 were used. In another set, these samples were stained oppositely, by Cy5 and Cy3, respectively.

Each of two identical antibody microarrays (GRAA2 components) contains 224 antibody spots organized in 16 sub-arrays and immobilized on the nitrocellulose-coated glass slide. Each sub-array has duplicate spots of 7 antibodies against various proteins involved in epigenetic modifications. Additionally, these sub-arrays contain a single spot with non-labeled bovine serum albumin (BSA) as a negative control and a single spot with Cy3 and Cy5-conjugated BSA as a positive control.

Microarray slides were incubated 40 min at a room temperature on a rocking shaker with 5 ml of the Array Incubation Buffer (GRAA2 component) containing the mixture of both: the experimental sample stained with Cy3 and the control sample stained with Cy5 at equal protein concentrations (10 μg/ml). Cy3 and Cy5 fluoresce in different spectral regions (532 and 635 nm, respectively), so that these samples can be easily distinguished on their fluorescence. Another microarray slide was incubated with the oppositely stained samples: Cy5 and Cy3, respectively. Such swapped staining provided verification of results and compensation of a potential bias in binding of Cy3 or Cy5 dyes to protein samples. This provides the double test and full self-control of the experiment. After following triple washing in the Washing buffer (GRAA2 component) and triple washing in pure water, the microarray slides were air dried overnight in the dark.

The microarrays were scanned using the GenePix 4100A Microarray Scanner (Molecular Devices, Sunnyvale, USA) at 532 and 635 nm (fluorescence maximums of Cy3 and Cy5, respectively). The fluorescence images were analyzed using the GenePix Pro 6.0 software. The ratio of the median fluorescence intensity in each spot of experimental samples (minus background fluorescence in the ring around the spot) to that of control samples indicated changes in the levels of proteins from photosensitized cerebral cortex relatively to control samples (the cerebral cortex tissue without ALA administration taken at the same time after irradiation). The GenePix Pro 6.0 method of normalization of the experimental data was used. This corrects the bias associated with different protein and bound dye content so that the data distribution is centered on 1. Two samples labeled in duplicate independently and reversely provided 4 experimental values for each protein. Experiments were duplicated. These values were averaged and standard deviations were determined. We used 30% cut-off level, i.e. only the experimental values differed from control by 30% or more were taken into account and interpreted. Although more than twofold difference (>100%) is often considered to be more reliable for interpretation of genomic data (in which thousands genes are analyzed), the 30% cut-off levels in the microarray proteomic experiments (that operate with only 100–200 proteins) allows involving into interpretation much more cellular proteins than 100% cut-off. This makes the picture more complete and logical. The validation and reliability of the proteomic microarray data are provided by the self-control experiment using the swapped staining in the second microarray.

3. Results

3.1. PpIX accumulation in the mouse cerebral cortex

The fluorescence spectrum (λ_{ex} = 406 nm) of PpIX dissolved in the extraction mixture with 5% HCl contained the sharp pike at 600–605 nm and the shoulder at 700–710 nm (Fig. 1) like in papers [21]. The control mouse cerebral cortex contained 1.2 ± 0.2 nmol/g tissue (n = 5) of endogenous PpIX that was in agreement with the data of other authors [17,22]. At 4 h after ALA administration (100 mg/kg, i.p.), PpIX level in the mouse cerebral cortex increased up to 3.1 ± 0.3 nmol/g tissue ($p < 0.01$; n = 5) relatively to control animals.

3.2. PDT-induced pathohistological changes

In the absence of ALA administration, laser irradiation (633 nm, 15 mW/cm^2, 20 min) did not induce significant morphological changes in the mouse cerebral cortex at 1 or 4 h post-treatment (Fig. 2A) as compared with untreated but operated mice. This group of animals was used as a control in further experiments. In contrast, ALA-PDT noticeably influenced the cerebral tissue morphology. At 1 h after ALA-PDT some neurons within the irradiated zone became hyperchromic, or hypochromic; some cells contained pyknotic nuclei. At the same time, others retained the normal morphology (Fig. 2B). The number of hyperchromic neurons increased by 4.5 times ($p < 0.01$), but numbers of hypochromic or pyknotic neurons did not change (Table 1). This represents the initial stage of brain injury.

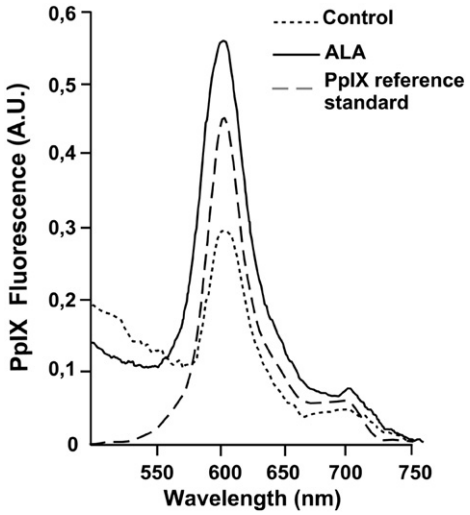

Fig. 1. Fluorescence spectra of protoporphyrin IX (λ_{ex} = 406 nm) in the mouse cerebral cortex at 4 h after i.p. administration of 100 mg/kg ALA (solid line) or without ALA (dotted line). Reference standard: 1 nmol/ml (dashed line).

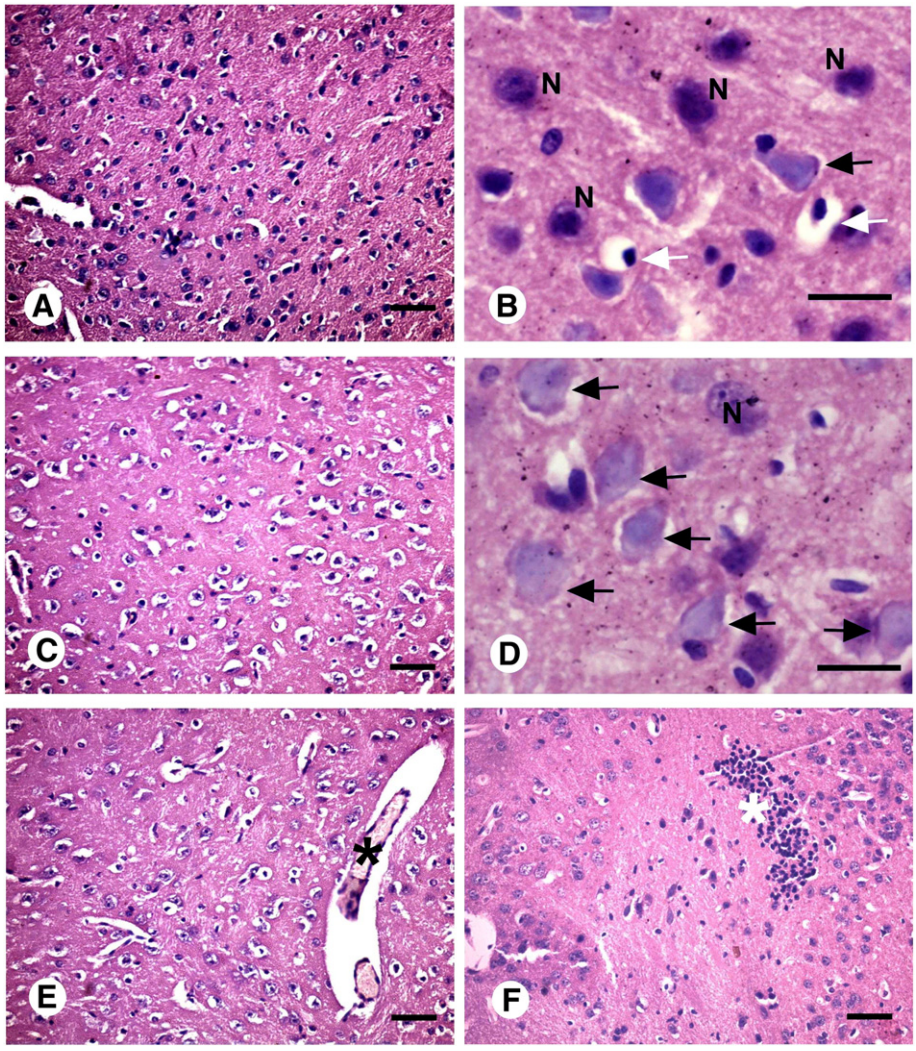

Fig. 2. ALA-PDT-induced changes in morphology of the mouse brain cortex. Hematoxylin–eosin staining. A) Untreated control prepair. B) The pyramid cortex layer at 1 h after ALA-PDT. White arrows show pyknotic neurons, black arrow — karyolysis. N — normal pyramid neurons. C–H) The pyramid cortex layer at 4 h after ALA-PDT. C) Cells at different death stages; loss of neurons. D) Karyolysis of neurons (black arrows). E) The blood vessels are filled with elements of plasma. Perivascular space is expanded. F) The glial infiltration region. Scale bar is 50 μm in all figures.

At 4 h after ALA-PDT, morphological alterations became more significant and characteristic for the late injury stages (Fig. 2C). Karyolysis and karyopyknosis occurred in some neuronal cells. Some "ghost neurons", which lost the affinity to hematoxylin, were observed (Fig. 2D). Such alterations were most significant in the cerebral pyramid neuron layer. At this time, the number of normal neurons decreased about 3 times but numbers of hyperchromic, hypochromic and pyknotic neurons substantially increased (Table 1). Blood vessels in the irradiation zone contained the expanded perivascular areas. Some vessels were filled with blood plasma that indicated the impaired microcirculation (Fig. 2E). Local infiltrations of glial cells (Fig. 2F) were observed in the upper cortex layers. Infiltrations of lymphocytes and macrophages also occurred. Notably, some normal cortex areas were present between necrotic zones. Thus, ALA-PDT killed some but not all neurons and caused limited microcirculatory alteration in the normal mouse cerebral cortex.

The gallocyanin–chromalum staining showed decrease in the RNA level in the nucleoli and cytoplasm of pyramid neurons at 1 and, especially, at 4 h after ALA-PDT (Fig. 3) that indicates the general suppression of biosynthetic processes.

Table 1
The number of normal and altered neurons stained with hematoxylin/eosin in the mouse sensomotory cortex at 1 or 4 h after ALA-PDT. Mean numbers of neurons (±SEM) were determined in six randomized fields in each slide. All groups consisted of 5 animals.

	Normal neurons	Hypochromic neurons	Hyperchromic neurons	Pyknotic neurons	Total number of neurons per visual field
Control	146 ± 20	12 ± 3	4 ± 1	7 ± 2	169 ± 23
ALA-PDT, 1 h	122 ± 13	14 ± 3	18 ± 6**	9 ± 2	162 ± 13
ALA-PDT, 4 h	49 ± 12**	36 ± 9*	57 ± 13**	27 ± 8*	168 ± 10

Significant difference from control group.
* $p < 0.05$.
** $p < 0.01$.

3.3. PDT-induced changes in expression of proteins involved in epigenetic regulation

More than 30% changes in the expression of some proteins involved in epigenetic regulation in the mouse cerebral cortex at different time intervals after ALA-PDT are shown in Table 2.

At 1 h after PDT we observed increase in the levels of phosphorylation of histone H2AX at serine 139 (γH2AX) and dimethylation of

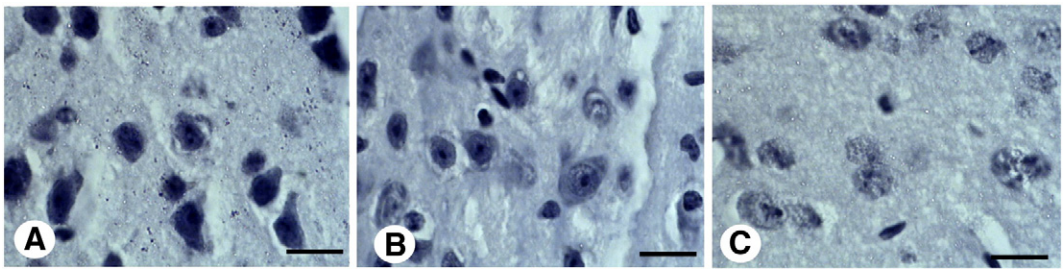

Fig. 3. Detection of nucleic acids in pyramid neurons in the mouse sensomotory cortex. Gallocyanin–chromalum staining. A) Control; B) 1 h after ALA-PDT; C) 4 h after ALA-PDT. Scale bars — 50 μm.

histone H3 at lysine 9 (H3K9me2) by 35–37%. The expression of histone deacetylases HDAC-1 and HDAC-11 increased by 33–36%, whereas the level of HDAC-10 decreased by 51%. We also observed 35% increase in the level of CENP-E (centromere protein E) involved in mitotic separation of chromosomes. The level of DNA methyl-binding protein Kaiso increased by 31% (Table 1). At the same time, the expression of PABP (poly(A)-binding protein) that is involved in transcription termination and provides stability and translation of mRNA in the cytoplasm, PML (promyelocytic leukemia), which participates in DNA replication and repair and regulates apoptosis, forkhead family transcription factor FOXC2 that regulates multiple key processes including differentiation, apoptosis, embryogenesis, and carcinogenesis, hABH1, a mitochondrial protein that demethylates 3-methylcytosine in single-stranded DNA and RNA, were down-regulated by 38–50%. Stronger decrease by 1.75–2.08 times demonstrated histone methyltransferases G9a and SUV39H1, which methylate lysine 9 in histone H3 and thereby induce gene silencing, and MTA1/MTA1L1 (metastasis-associated protein 1/metastasis tumor associated 1-like 1) that interacts with HDAC-1 and thereby participates in transcriptional repression.

More than 5-fold overexpression of transcription factor AP-1/c-Jun was the biggest change among the studied proteins at 4 h after ALA-PDT. The expression of arginine methyltransferase PRMT5, importin α5/7 and transcription factor E2F4 increased by 30–37%, whereas at 1 h after PDT their expression exceeded the control levels only by 8–26% (Table 2). On the other hand, the overexpression of γH2AX, H3K9me2, CENP-E was diminished and almost approached the control levels. However, the down-regulation of BACH1 (breast cancer type 1 protein), histone deacetylase SIR 2, and chromatin-remodeling factor hBrm/hsnf2a became higher and reached 30–38%. The difference between expression of PABP, PML, FOXC2, G9a, MTA1/MTA1L1 and SUV39H1 in the PDT-treated and control brain tissues was less compared to 1 h after ALA-PDT. Nevertheless, the expression of G9a, MTA1/MTA1L1 and SUV39H1 remained 1.5 times higher than in control samples. At 4 h after ALA-PDT the levels of HDAC-1, HDAC-10, HDAC-11, Kaiso, hABH1, and importin α5/7 changed insignificantly (<10%) compared to 1 h interval (Table 2).

3.4. Immunohistochemical detection of HDAC-1 and H3K9me2 in the PDT-treated mouse cerebral cortex

At 1 h after ALA-PDT, the immunoreactivity of HDAC-1 and H3K9me2 in the mouse cerebral cortex increased by 44 and 33%: from 12.1 ± 1.5% to 17.4 ± 2.1% ($p < 0.05$) and from 6.1 ± 0.6% to 8.1 ±1.0% ($p < 0.05$), respectively (Fig. 4).

4. Discussion

Blood–brain barrier limits penetration of ALA into the normal brain tissue and following PpIX production [23]. Nevertheless, i.p. administration of ALA caused 2.5-fold increase in the PpIX level to 3.1 nmol/g tissue (or 1.7 μg/g) in the normal mouse cerebral cortex as compared to its background level (1.2 nmol/g tissue, or 0.7 μg/g). This is in agreement

Table 2
More than 30% increase (experimental/control group) or decrease (control/experimental group) of the level of epigenetic proteins in the mouse cerebral cortex at 1 and 4 h after ALA-PDT as compared to the control levels.

Name	1 h		4 h		Protein function
	Mean	SD	Mean	SD	
Exp/Ctr (up-regulation)					
Phosphorylated histone H2AX (pSer139)	1.37	0.04	1.21	0.02	Phosphorylation of serine139 in histone H2AX; a marker of double-strand DNA breaks
HDAC-11	1.36	0.02	1.28	0.02	Histone deacetylase. Inhibits gene expression
Dimethylated histone H3 (H3K9me2)	1.35	0.07	1.20	0.05	Methylation of lysine 9 in histone H3 leads to epigenetic gene silencing
CENP-E	1.35	0.02	1.06	0.03	mitotic separation of chromosomes
HDAC-1	1.33	0.13	1.30	0.22	Histone deacetylase. Inhibits gene expression
Kaiso	1.31	0.06	1.27	0.01	DNA methyl-binding protein. Transcription repressor
PRMT5	1.26	0.08	1.37	0.01	Arginine methyl transferase. Regulates signal transduction, transcription and splicing
Importin α5/7	1.23	0.09	1.34	0.04	Nuclear protein import
AP-1/c-Jun	1.08	0.04	5.43	2.37	Activation Protein transcription factor 1 (AP-1)
E2F4	1.10	0.04	1.30	0.24	Transcription factor. Regulation of proliferation
Ctr/Exp (down-regulation)					
BACH1	1.16	0.02	1.31	0.07	Breast cancer type1 protein: C-terminal helicase
SIR 2	1.20	0.11	1.30	0.05	NAD-dependent histone deacetylase. Removes acetyl groups from histone lysines
hBrm/hsnf2a	1.27	0.08	1.38	0.07	Chromatin remodeling factor; activates transcription
PABP	1.38	0.07	1.14	0.06	Poly(A)-binding protein. Involved in transcription termination.
PML	1.41	0.15	1.27	0.16	Involved in DNA replication and reparation. Protects p53 from degradation. Regulates apoptosis.
FOXC2	1.44	0.08	1.31	0.08	Forkhead family transcription factor. Regulates cell differentiation, apoptosis, embryogenesis, carcinogenesis
hABH1	1.50	0.22	1.50	0.30	Demethylates 3-methylcytosine in mitochondrial DNA and RNA.
HDAC-10	1.51	0.09	1.41	0.16	Histone deacetylase. Inhibits gene expression
G9a methyltransferase	1.75	0.05	1.50	0.29	Histone methyltransferase; methylates Lys-9 in histone H3
MTA1/MTA1L1	1.93	0.34	1.47	0.11	Links corepressor complexes and the general transcription machinery

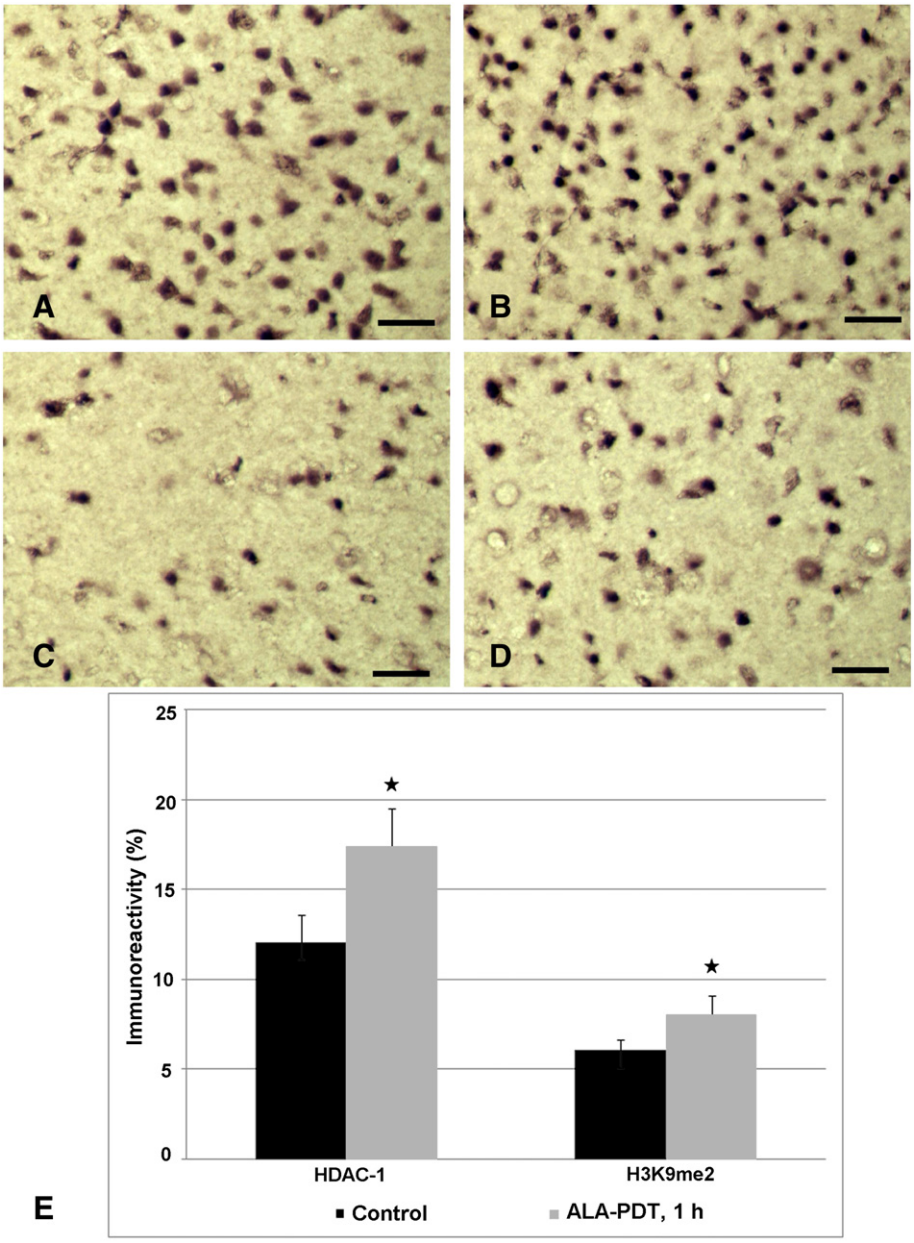

Fig. 4. ALA-PDT-induced changes in the HDAC-1 and H3K9me2 immunoreactivity in the mouse cerebral cortex. A) HDAC-1; control mouse. B) HDAC-1; PDT-treated mouse (1 h after ALA-PDT). C) H3K9me2; control mouse. D) H3K9me2; PDT-treated mouse (1 h after ALA-PDT). Objective 40×. Scale bars — 50 μm. E) The immunoreactivity indexes of HDAC-1 and H3K9me2 (mean ± SD) in the experimental and control groups (12 sections in each of 3 experimental and 3 control mice were examined). * — $p < 0.05$.

with PpIX accumulation in the brain tissue of normal mice but several times lower than in tumor-bearing mice [17] and patients [6]. Brain tumors accumulate more ALA-induced PpIX due to disruption of blood–brain barrier and more efficient enzymatic pathways as compared with normal tissue [4,24,25].

ALA-PDT injured the nervous tissue. Morphological alterations including blood vessel impairments and cell death developed in the photosensitized mouse cerebral cortex at 1 h and, more significantly, at 4 h after the treatment. PDT-induced formation and enlargement of endothelial gaps in cerebral vessels and brain edema were also observed by other authors [20]. Disruption of the blood–brain barrier by ALA-PDT exacerbates injury of the nervous tissue [24]. As shown *in vitro*, ALA-PDT induces massive apoptosis mediated by the mitochondrial proapoptotic pathway in glioma cell lines [26,27]. However, other authors showed that ALA-PDT induces predominately necrosis in various glioma cell lines and spheroids [28], glioblastoma tissue [29], and normal rabbit brain [30]. Seldom apoptotic cells were observed near the regions of coagulative necrosis [30]. As reported by Lilge et al., PDT-induced necrosis resulted from direct oxidative cell injury, whereas apoptosis could be associated with secondary effects such as vascular damage, edema, and hypoxia [30]. The results of our histological study are in agreement with these data. The number of normal neurons progressively decreased after ALA-PDT. At the same time, the number of pathologically altered cells (pyknotic, hypo- or hyperchromic) increased at 4 h after the treatment. The level of nucleic acid (mainly RNA) in cytoplasm and nucleoli also decreased. These observations correspond to general PDT-induced injury of the brain tissue. Nevertheless, some cell protection reactions occur along with injurious processes. Epigenetic regulations play an important role in both cell survival and death.

Epigenetic processes are involved in the oxidative injury of the nervous tissue [31]. However, their role in PDT-induced normal brain damage remains unstudied. According to our data, ALA-PDT influenced the

expression of some proteins involved in epigenetic regulation of transcription, DNA repair, nuclear protein transport, proliferation, and cell survival in the cerebral cortex of normal mice. These changes depended on the time interval after the treatment. Expression of some proteins changed only at 1 h after PDT, others — at 4 h; some proteins were up- or down-regulated during both intervals.

4.1. Transcription regulation

Transcriptional activity is regulated at the epigenetic level by cytosine methylation of gene promoters or covalent histone modifications. At 1 h after ALA-PDT we observed changes in the expression of diverse epigenetic proteins leading to overall suppression of transcriptional activity in the mouse cerebral cortex. Although the microarray technology does not estimate DNA methylation, we observed 31% up-regulation of DNA methylation-dependent transcriptional repressor Kaiso, which recruits the HDAC-containing co-repressor complex N-CoR to methylated sites in the genome [32]. This represses transcription of target genes involved in some signaling pathways (i.e. Wnt). The 38% decrease in the level of PABP, which participates in transcription termination [33], and 44% down-regulation of transcription factor FOXC2 also indicated the negative regulation of gene transcription in the photosensitized cerebral cortex. Since FOXC2 directly regulates the expression of some genes involved in angiogenesis [34], one can suggest that its down-regulation is related to microvascular remodeling in the photosensitized brain that was observed in our histological study. The 38% down-regulation of chromatin remodeling factor hBrm/hsnf2a that activates transcription indicated the delayed (at 4 h after PDT) suppression of transcriptional activity in the mouse cerebral cortex.

4.2. Histone modifications

Histone modifications represent another level of transcriptional regulation. The 35% overexpression of dimethylated histone H3 that leads to long-term transcriptional repression [35] was observed at 1 h after ALA-PDT. This data was confirmed in the immunohistochemical experiments. However, the levels of histone methyltransferases G9a and SUV39H1, which methylate lysine 9 in histone H3 [36], significantly decreased by 1.8 and 2.1 times at 1 h after ALA-PDT and remained 1.5-fold increased at 4 h. Histone H3 could be rapidly methylated within the first hour after PDT, and the unnecessary enzymes degraded later.

Histone acetylation involved in chromatin unpacking stimulates transcription and gene expression. Oppositely, histone deacetylation suppresses transcription [36]. ALA-PDT induced up-regulation of histone deacetylases HDAC-1 and HDAC-11 by 28–36% and down-regulation of HDAC-10 by 41–51% at 1–4 h after the treatment. The difference between responses of various HDACs to PDT could be associated with their different localization and functions in the nervous system. HDAC-1 and -11 are widely expressed in the mammalian brain including cerebral cortex. HDAC-1 resides mainly in the cell nuclei, whereas HDAC-11 has dual, nuclear and cytoplasmic, localization [37,38]. In the mouse brain HDAC-11 is especially expressed in the nuclei of mature oligodendrocytes but not astrocytes [39]. Since glia is the major part of the mammalian cerebral cortex, one can suggest that the up-regulation of HDAC-11 in the photosensitized mouse cerebral cortex represented mainly the oligodendroglial response, whereas the up-regulation of HDAC-1 was possibly the neuronal response. This suggestion was confirmed in the immunohistochemical study. HDAC-1 is known as a molecular switch between neuronal survival and death. Its activity depends on inclusion into the multiprotein chromatin-remodeling complex. For example, its interaction with HDAC-related protein (HDRP) promotes neuronal survival, whereas interaction with HDAC-3 leads to cell death [40].

HDAC-10 is found in the nuclei and the cytoplasm of dopamine and noradrenaline neurons [34], which do not reside in the cerebral cortex. The cortical HDAC-10 could possibly present in axons of these neurons, which are spreading throughout the brain, or in glial cells. Its functions in neuronal cells are still unknown. However, as shown in human cancer cells, down-regulation of HDAC-10 can induce expression of thioredoxin-interacting protein (TXNIP), accumulation of reactive oxygen species, release of cytochrome c and apoptosis [41]. One can suggest the similar role of HDAC-10 in PDT-treated mouse brain, where its down-regulation could exacerbate oxidative tissue damage.

At 4 h after ALA-PDT we observed 30% decrease in the level of NAD-dependent histone deacetylase SIR2, which mediates chromatin silencing and links cellular metabolism and transcriptional activity. Sirt1, the mammalian homolog of SIR2, is known to regulate cell resistance to oxidative stress and prevent apoptosis [42]. Down-regulation of SIR-2 in our experiments could indicate a slow decrease in the resistance of brain tissue to PDT-induced oxidative stress.

4.3. Proteins involved in DNA repair

Changes in DNA repair and transcription regulation were among the first responses of the brain tissue to photodynamic treatment. PDT does not induce DNA breaks by itself because PpIX does not penetrate into the cell nucleus [43]. However, PDT stimulates apoptotic DNA fragmentation. The present experiments showed significant down-regulation of MTA1/MTA1L1 by 93 and 47% at 1 and 4 h after ALA-PDT, respectively. This protein is involved in DNA repair, regulation of cell resistance, and early apoptosis stages [44]. The level of PML, which also participates in DNA repair, was decreased by 41% at 1 h after PDT. PML induction is known to precede DNA fragmentation in neurons at 1 h after ischemic damage [45]. The 50% down-regulation of a mitochondrial protein hABH1 was observed at 1 and 4 h after PDT. This protein demethylates 3-methylcytosines in mitochondrial DNA and RNA. hABH-mediated base repair increases survival of glia cells [46]. The observed down-regulation of MTA1/MTA1L1, PML, and hABH1 indicates impairment of the DNA repair complex. As a result, phosphorylated histone H2AX (γH2AX) that participates in the double-strand break DNA repair was up-regulated by 37%. This signals about DNA breaks and initiates the assembly of DNA repair complex. The level of γH2AX is known to be increased under UV radiation and at early stages of apoptosis, but decreased gradually during apoptosis progression [47]. ALA-PDT-induced overexpression of γH2AX in the present work indicated the appearance of double-strand DNA breaks.

4.4. Proteins involved in cell proliferation

The first observed alteration in the expression of a protein involved in regulation of the cell cycle was 35% up-regulation of centromere protein E (CENP-E), which participates in mitotic separation of chromosomes, at 1 h after ALA-PDT. At 4 h post-treatment, we observed 30% up-regulation of transcription factor E2F4, which controls proliferation of neuronal cells [48]. This data correlated with 37% up-regulation of arginine methyltransferase PRMT5, which methylates arginines in cytoplasmic proteins and thereby regulates signal transduction, transcription, splicing and RNA transport. Being associated with chromatin remodeling complex hSWI/SNF, PRMT5 negatively controls transcription of growth inhibitory genes. Therefore, its overexpression stimulates proliferation and promotes tumor growth [49]. The level of importin α5/7 was increased simultaneously by 34%. This protein participates in the import of transcription factors such as NF-κB and following elevated transcription of genes involved into anti-apoptotic protection and cell proliferation [50]. Thus, ALA-PDT induces proteins involved in epigenetic stimulation of the cell proliferation in the cerebral cortex. Since neurons do not proliferate, this process may be related to proliferation of glial cells, named as reactive gliosis.

4.5. Proteins involved in regulation of cell death

c-Jun protein, a component of activation protein transcription factor 1 (AP-1), is involved in regulation of cell proliferation, differentiation,

responses to stress factors and apoptosis. Overexpression of c-Jun is involved in apoptosis in neuronal cells [51]. More than 5-fold overexpression of AP-1/c-Jun at 4 h after ALA-PDT was the most significant change among the studied proteins. This data may indicate to promotion of apoptotic processes in the mouse cerebral cortex at 4 but not 1 h after ALA-PDT.

On the other hand, the 31% down-regulation of BACH1 (breast cancer type1 protein), a transcriptional repressor of the heme oxigenase-1 gene, was observed at this moment. Its down-regulation results in production of heme oxigenase-1 that plays a critical role in tissue protection from oxidative stress [52]. Therefore, two opposite tendencies directed to cell survival and cell death are developed simultaneously in the photosensitized mouse cerebral cortex.

These results are summarized in Fig. 5.

4.6. General comments

The advantage of the microarray technology is the capability to evaluate simultaneous changes in the expression of hundreds and thousands proteins or genes in the same experimental or clinical material. However, the consistence of the data obtained in different laboratories is limited due to fragmentary information on various cellular processes. Because of too high the cut-off level, some significant proteins are not considered [53]. Cell functions are regulated by coordinated activity of numerous interacting signaling pathways. Therefore, the comprehensive evaluation of coherent changes in the complex massive of proteins involved in various signaling pathways and epigenetic processes significantly increases understanding of the inner logics of cellular processes and elevates the reliability and reasonability of biologically valuable conclusions [54,55]. The proteomic, like genomic data are rather descriptive. They list proteins with altered expression and point out to possible participants of the studied pathological process. However, they do not disclose the reasons of changes in their expression because the signaling pathways and transcription factors that control production of these proteins remain unknown. Further mechanistic investigations should reveal the signaling and metabolic pathways that regulate production, transport, processing and degradation of these proteins. Nevertheless, the obtained results may indicate possible markers and targets for diagnosis and treatment of oxidative brain injury.

Thus, our experiments demonstrated that ALA-PDT kills some but not all neuronal cells and causes microvascular alterations in the normal mouse cerebral cortex. Using proteomic microarrays, we showed that ALA-PDT induced changes in the expression of some proteins involved in epigenetic regulation and histone modifications directed to suppression of transcriptional activity, inhibition of DNA repair, stimulation of proliferation, nuclear protein import, and regulation of cell survival and apoptosis in the mouse cerebral cortex. These changes depended on the time interval after PDT. Major alterations observed in the first hour after the treatment resulted in suppression of transcription and DNA repair. At 4 h after PDT the expression of proteins involved in regulation of proliferation or death of cortical cells changed more significantly.

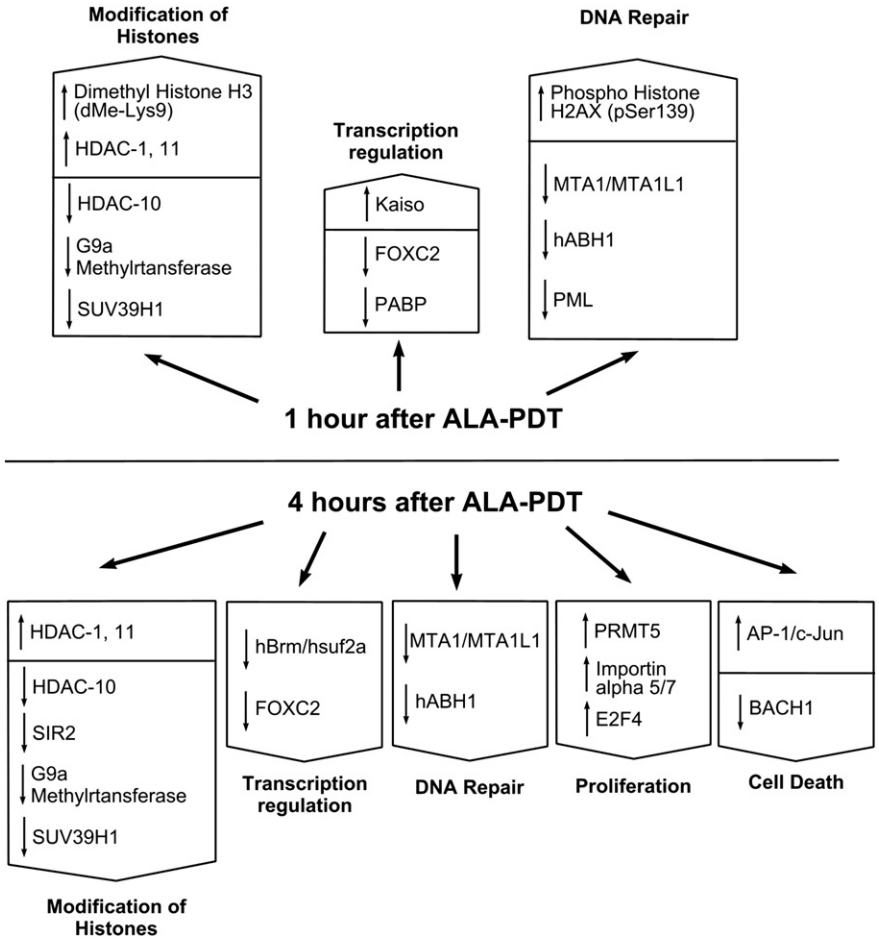

Fig. 5. Changes in the expression of proteins involved in epigenetic regulation in the mouse cerebral cortex at 1 or 4 h after ALA-PDT.

Acknowledgements

The work was supported by grants of RFBR (11-04-01476), Minobrnauki of Russia (No. 4.6142.2011) and Southern Federal University.

References

[1] P. Agostinis, K. Berg, K.A. Cengel, T.H. Foster, A.W. Girotti, S.O. Gollnick, S.M. Hahn, M.R. Hamblin, A. Juzeniene, D. Kessel, M. Korbelik, J. Moan, P. Mroz, D. Nowis, J. Piette, B.C. Wilson, J. Golab, Photodynamic therapy of cancer: an update, CA Cancer J. Clin. 61 (2011) 250–281.
[2] A. Juzeniene, J. Moan, The principles of 5-aminolevulinic acid photodynamic therapy, in: A.B. Uzdensky (Ed.), Photodynamic therapy at the cellular level, Research Signpost, Trivandrum, 2007, pp. 115–140.
[3] H. Kostron, Photodynamic diagnosis and therapy and the brain, Methods Mol. Biol. 635 (2010) 261–280.
[4] H. Stepp, T. Beck, T. Pongratz, T. Meinel, F.W. Kreth, J.C. Tonn, W. Stummer, ALA and malignant glioma: fluorescence-guided resection and photodynamic treatment, J. Environ. Pathol. Toxicol. Oncol. 26 (2007) 157–164.
[5] S.J. Madsen, E. Angell-Petersen, S. Spetalen, S.W. Carper, S.A. Ziegler, H. Hirschberg, Photodynamic therapy of newly implanted glioma cells in the rat brain, Lasers Surg. Med. 38 (2006) 540–548.
[6] S.S. Stylli, A.H. Kaye, Photodynamic therapy of cerebral glioma — a review. Part II. — clinical studies, J. Clin. Neurosci. 13 (2006) 709–717.
[7] B. Gomperts, I. Kramer, P. Tatham, Signal Transduction, Elsevier, Academic Press, Amsterdam et al., 2009
[8] E. Buytaert, M. Dewaele, P. Agostinis, Molecular effectors of multiple cell death pathways initiated by photodynamic therapy, Biochim. Biophys. Acta 1776 (2007) 86–107.
[9] A.B. Uzdensky, Signal transduction and photodynamic therapy, Curr. Signal Transduct. Ther. 3 (2008) 55–74.
[10] F.A. Sultan, J.J. Day, Epigenetic mechanisms in memory and synaptic function, Epigenomics 3 (2011) 157–181.
[11] N.H. Zawia, D.K. Lahiri, F. Cardozo-Pelaez, Epigenetics, oxidative stress, and Alzheimer disease, Free Radic. Biol. Med. (46) (2009) 1241–1249.
[12] S.G. Gray, Epigenetic treatment of neurological disease, Epigenomics 3 (2011) 431–450.
[13] P.J. Gebicke-Haerter, Epigenetics of schizophrenia, Pharmacopsychiatry 45 (2012) S42–S48.
[14] J.Y. Hwang, K.A. Aromolaran, R.S. Zukin, Epigenetic mechanisms in stroke and epilepsy, Neuropsychopharmacology 38 (2013) 167–182.
[15] S.L. Gibbs-Strauss, J.A. O'Hara, P.J. Hoopes, T. Hasan, B.W. Pogue, Noninvasive measurement of aminolevulinic acid-induced protoporphyrin IX fluorescence allowing detection of murine glioma in vivo, J. Biomed. Opt. 14 (2009) 540–548.
[16] C. Perotti, A. Casas, H. Fukuda, P. Sacca, A. Batlle, ALA and ALA hexyl ester induction of porphyrins after their systemic administration to tumour bearing mice, Br. J. Cancer 87 (2002) 790–795.
[17] G. Di Venosa, A. Batlle, H. Fukuda, A. Macrobert, A. Casas, Distribution of 5-aminolevulinic acid derivatives and induced porphyrin kinetics in mice tissues, Cancer Chemother. Pharmacol. 58 (2006) 478–486.
[18] L. Einarson, On the theory of gallocyanin–chromalum staining and its application for quantitative estimation of basophilia; a selective staining of exquisite progressivity, Acta Pathol. Microbiol. Scand. 28 (1951) 82–102.
[19] D.A. Cruz, S.M. Eggan, D.A. Lewis, Postnatal development of pre- and postsynaptic GABA markers at chandelier cell connections with pyramidal neurons in monkey prefrontal cortex, J. Comp. Neurol. 465 (2003) 385–400.
[20] M.S. Mathews, D. Chighvinadze, H.M. Gach, F.A. Uzal, S.J. Madsen, H. Hirschberg, Cerebral edema following photodynamic therapy using endogenous and exogenous photosensitizers in normal brain, Lasers Surg. Med. 43 (2011) 892–900.
[21] C.S. Loh, D. Vernon, A.J. Macrobert, J. Bedwell, S.G. Bown, S.B. Brown, Endogenous porphyrin distribution induced by 5-aminolaevulinic acid in the tissue layers of the gastrointestinal tract, J. Photochem. Photobiol. B 20 (1993) 47–54.
[22] J. Van den Boogert, R. van Hillegersberg, F.W. de Rooij, R.W. de Bruin, A. Edixhoven-Bosdijk, A.B. Houtsmuller, P.D. Siersema, J.H. Wilson, H.W. Tilanus, 5-Aminolaevulinic acid-induced protoporphyrin IX accumulation in tissues: pharmacokinetics after oral or intravenous administration, J. Photochem. Photobiol. B 44 (1998) 29–38.
[23] S.R. Ennis, A. Novotny, J. Xiang, P. Shakui, T. Masada, W. Stummer, D.E. Smith, R.F. Keep, Transport of 5-aminolevulinic acid between blood and brain, Brain Res. 959 (2003) 226–234.
[24] H. Hirschberg, F.A. Uzal, D. Chighvinadze, M.J. Zhang, Q. Peng, S.J. Madsen, Disruption of the blood-brain barrier following ALA-mediated photodynamic therapy, Lasers Surg. Med. 40 (2008) 535–542.
[25] M. Ishizuka, F. Abe, Y. Sano, K. Takahashi, K. Inoue, M. Nakajima, T. Kohda, N. Komatsu, S. Ogura, T. Tanaka, Novel development of 5-aminolevurinic acid (ALA) in cancer diagnoses and therapy, Int. Immunopharmacol. 11 (2011) 358–365.
[26] H. Inoue, Y. Kajimoto, M.A. Shibata, N. Miyoshi, N. Ogawa, S. Miyatake, Y. Otsuki, T. Kuroiwa, Massive apoptotic cell death of human glioma cells via a mitochondrial pathway following 5-aminolevulinic acid-mediated photodynamic therapy, J. Neurooncol. 83 (2007) 223–231.
[27] S. Karmakar, N.L. Banik, S.J. Patel, S.K. Ray, 5-Aminolevulinic acid-based photodynamic therapy suppressed survival factors and activated proteases for apoptosis in human glioblastoma U87MG cells, Neurosci. Lett. 415 (2007) 242–247.
[28] Y. Kamashima, S. Terasaka, S. Kuroda, Y. Iwasaki, Morphological and histological changes of glioma cells immediately after 5-aminolevulinic acid mediated photodynamic therapy, Neurol. Res. 33 (2011) 739–746.
[29] I. Coupienne, G. Fettweis, N. Rubio, P. Agostinis, J. Piette, 5-ALA-PDT induces RIP3-dependent necrosis in glioblastoma, Photochem. Photobiol. Sci. 10 (2011) 1868–1878.
[30] L. Lilge, M. Portnoy, B.C. Wilson, Apoptosis induced in vivo by photodynamic therapy in normal brain and intracranial tumour tissue, Br. J. Cancer 83 (2008) 1110–1117.
[31] A.R. Cyr, F.E. Domann, The redox basis of epigenetic modifications: from mechanisms to functional consequences, Antioxid. Redox Signal. 15 (2011) 551–589.
[32] H.G. Yoon, D.W. Chan, A.B. Reynolds, J. Qin, J. Wong, N-CoR mediates DNA methylation-dependent repression through a methyl CpG binding protein Kaiso, Mol. Cell 12 (2003) 723–734.
[33] A. Kahvejian, G. Roy, N. Sonenberg, The mRNA closed-loop model: the function of PABP and PABP-interacting proteins in mRNA translation, Cold Spring Harb. Symp. Quant. Biol. 66 (2001) 293–300.
[34] T. Kume, FOXC2 transcription factor: a newly described regulator of angiogenesis, Trends Cardiovasc. Med. 18 (2008) 224–228.
[35] R. Margueron, P. Trojer, D. Reinberg, The key to development: interpreting the histone code? Curr. Opin. Genet. Dev. 15 (2005) 163–176.
[36] C.D. Allis, T. Jenuwein, D. Reinberg, Epigenetics, Cold Spring Harbor Laboratory Press, Cold Spring Harbor, New York, 2006.
[37] Y.T. Chen, X.F. Zang, J. Pan, X.L. Zhu, F. Chen, Z.B. Chen, Y. Xu, Expression patterns of histone deacetylases in experimental stroke and potential targets for neuroprotection, Clin. Exp. Pharmacol. Physiol. 39 (2012) 751–758.
[38] K. Takase, S. Oda, M. Kuroda, H. Funato, Monoaminergic and neuropeptidergic neurons have distinct expression profiles of histone deacetylases, PLoS One 8 (2013) e58473.
[39] H. Liu, Q. Hu, A. Kaufman, A.J. D'Ercole, P. Ye, Developmental expression of histone deacetylase 11 in the murine brain, J. Neurosci. Res. 86 (2008) 537–543.
[40] F.H. Bardai, V. Price, M. Zaayman, L. Wang, S.R. D'Mello, Histone deacetylase-1 (HDAC1) is a molecular switch between neuronal survival and death, J. Biol. Chem. 287 (2012) 35444–35453.
[41] J.H. Lee, E.G. Jeong, M.C. Choi, S.H. Kim, J.H. Park, S.H. Song, J. Park, Y.J. Bang, T.Y. Kim, Inhibition of histone deacetylase 10 induces thioredoxin-interacting protein and causes accumulation of reactive oxygen species in SNU-620 human gastric cancer cells, Mol. Cells 30 (2010) 107–112.
[42] R.R. Alcendor, S. Gao, P. Zhai, D. Zablocki, E. Holle, X. Yu, B. Tian, T. Wagner, S.F. Vatner, J. Sadoshima, Sirt1 regulates aging and resistance to oxidative stress in the heart, Circ. Res. 100 (2007) 1512–1521.
[43] S.M. Wu, Q.G. Ren, M.O. Zhou, Q. Peng, J.Y. Chen, Protoporphyrin IX production and its photodynamic effects on glioma cells, neuroblastoma cells and normal cerebellar granule cells in vitro with 5-aminolevulinic acid and its hexylester, Cancer Lett. 200 (2003) 123–131.
[44] D.Q. Li, K. Ohshiro, M.N. Khan, R. Kumar, Requirement of MTA1 in ATR-mediated DNA damage checkpoint function, J. Biol. Chem. 285 (2010) 19802–19812.
[45] T. Hayashi, C. Sasaki, M. Iwai, K. Sato, W.R. Zhang, K. Abe, Induction of PML immunoreactivity in rat brain neurons after transient middle cerebral artery occlusion, Neurol. Res. 23 (2001) 772–776.
[46] M.P. Westbye, E. Feyzi, P.A. Aas, C.B. Vågbø, V. Talstad, A. Warita, B. Kavli, L. Hagen, O. Sundheim, M. Akbari, N.B. Liabakk, G. Slupphaug, M. Otterlei, H.E. Krokan, Human AlkB homolog 1 is a mitochondrial protein that demethylates 3-methylcytosine in DNA and RNA, J. Biol. Chem. 283 (2008) 25046–25056.
[47] T. Tanaka, X. Huang, H.D. Halicka, H. Zhao, F. Traganos, A.P. Albino, W. Dai, Z. Darzynkiewicz, Cytometry of ATM activation and histone H2AX phosphorylation to estimate extent of DNA damage induced by exogenous agents, Cytometry A 71 (2007) 648–661.
[48] S.P. Persengiev, I.I. Kondova, D.L. Kilpatrick, E2F4 actively promotes the initiation and maintenance of nerve growth factor-induced cell differentiation, Mol. Cell. Biol. 19 (1999) 6048–6056.
[49] A. Scoumanne, J. Zhang, X. Chen, PRMT5 is required for cell-cycle progression and p53 tumor suppressor function, Nucleic Acids Res. 37 (2009) 4965–4976.
[50] R. Fagerlund, K. Melen, X. Cao, I. Julkunen, NF-kappaB p52, RelB and c-Rel are transported into the nucleus via a subset of importin alpha molecules, Cell. Signal. 20 (2008) 1442–1451.
[51] A. Behrens, M. Sibilia, E.F. Wagner, Amino-terminal phosphorylation of c-Jun regulates stress-induced apoptosis and cellular proliferation, Nat. Genet. 21 (1999) 326–329.
[52] E. Sakoda, K. Igarashi, J. Sun, K. Kurisu, S. Tashiro, Regulation of heme oxygenase-1 by transcription factor Bach1 in the mouse brain, Neurosci. Lett. 440 (2008) 160–165.
[53] J. Chen, Y. Wang, B. Shen, D. Zhang, Molecular signature of cancer at gene level or pathway level? Case studies of colorectal cancer and prostate cancer microarray data, Comput. Math. Methods Med. 2013 (2013) 909525.
[54] D.A. Hosack, G. Dennis Jr., B.T. Sherman, H.C. Lane, R.A. Lempicki, Identifying biological themes within lists of genes with EASE, Genome Biol. 4 (2003) R70.
[55] J. Zhu, J. Wang, Z. Guo, M. Zhang, D. Wang, Y. Li, D. Wang, G. Xiao, GO-2D: identifying 2-dimensional cellular-localized functional modules in Gene Ontology, BMC Genomics 8 (2007)(article 30).